Phosphorus containing carbon (submicron)fibers as efficient acid catalysts

Francisco J. García-Mateos, Ramiro Ruiz-Rosas, Juana Mª Rosas, José Rodríguez-Mirasol, Tomás Cordero*

Universidad de Málaga, Andalucia Tech., Departamento de Ingeniería química, Campus de Teatinos s/n, 29010, Málaga, Spain

Graphical Abstract

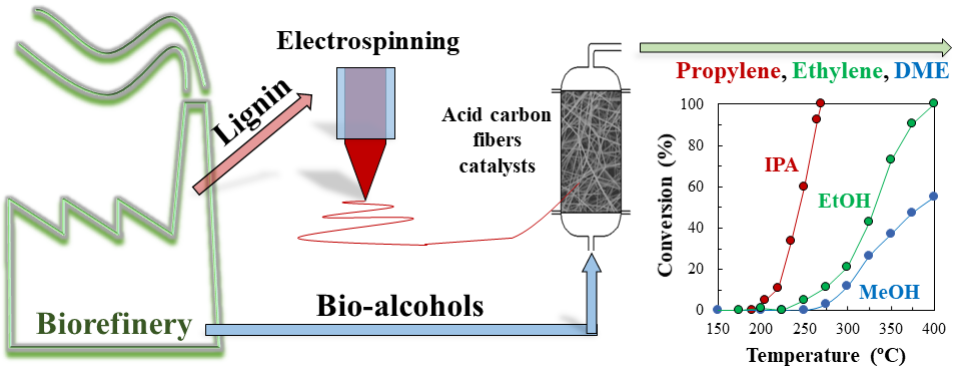

ABSTRACT

Porous carbon fibers catalysts have been prepared by electrospinning of Alcell lignin, a green carbon precursor, which could be obtained as by-product in wood-to-ethanol biorefineries. The addition of H_3PO_4, a well-known chemical activation agent, to the electrospinning lignin solutions, at different mass ratios and the use of different carbonization temperatures, between 500 and 1600 ºC, were analyzed in order to obtain carbon fibers with a large variety of porosity and chemical surface properties. Isopropanol decomposition was used as a catalytic test. Phosphorus-containing carbon fibers showed acid character and high catalytic activity, achieving propylene selectivity of 100 % under inert atmosphere. However, the use of air atmosphere increases the isopropanol conversion but produces the formation of acetone, via oxidative dehydrogenation, at low temperatures (~20%). Ethanol and methanol decomposition were also evaluated in air stream for the most active phosphorus-containing carbon catalyst, showing improved alcohol conversions with minimal gasification of the carbon fibers. These results confirmed that phosphorus-containing carbon fibers prepared by electrospinning of lignin solutions were excellent catalysts for alcohol dehydration reactions.

Keywords: activated carbon fibers; catalyst; electrospinning; H_3PO_4; alcohol dehydration

Notation

a'	specific area (m^{-1})
A_{BET}	apparent surface area measured by N_2 adsorption at -196 ºC (m^2 g^{-1})
ACF	activated carbon fibers
A_{DR}	narrow micropore surface area measured by CO_2 adsorption at 0 ºC (m^2 g^{-1})
BET	Brunauer, Emmett and Teller
Ca	Carberry number
C_b	bulk concentration (mol m^{-3})
DEE	diethyl ether
D_{eff}	effective diffusion coefficient (m^2 s^{-1})
DME	dimethyl ether
DR	Dubinin-Radushkevich
E_a	activation energy (kJ mol^{-1})
EDX	energy dispersive X-Ray
EtOH	ethanol
F_{0IPA}	initial isopropanol molar flow (μmol s^{-1})
h	heat transfer coefficient (J s^{-1} m^{-2} K^{-1})
ΔH_{IPA}	enthalpy of adsorption of isopropanol (kJ mol^{-1})
ΔH_{PROP}	enthalpy of adsorption of propylene (kJ mol^{-1})
ΔHr	reaction enthalpy (kJ mol^{-1})
IPA	isopropanol
k	apparent isopropanol rate constant (μmol atm^{-1} g^{-1} s^{-1})
k_0	preexponential factor (μmol atm^{-1} g^{-1} s^{-1})
k_g	mass transfer coefficient (m s^{-1})
k_{PROP}	propylene formation rate constant (mol g^{-1} s^{-1})
k_v	isopropanol rate constant (s^{-1})
K_{IPA}	isopropanol adsorption constant (atm^{-1})
K_{PROP}	propylene adsorption constant (atm^{-1})
MeOH	methanol
P_{0EtOH}	ethanol partial pressure (atm)
P_{0IPA}	isopropanol partial pressure (atm)
P_{0MeOH}	methanol partial pressure (atm)

PCFLs	phosphorus carbon fibers prepared with the lowest H_3PO_4/lignin ratio
PCFHs	phosphorus carbon fibers prepared with the highest H_3PO_4/lignin ratio
PROP	propylene
P_{PROP}	propylene partial pressure (atm)
Py	pyridine
Rf	carbon fibers radius (m)
r_{IPA}	isopropanol conversion rate (mol s^{-1} g^{-1})
r_{max}	maximum mass transfer rate (mol m^{-3}_{cat} s^{-1})
r_{obs}	observed reaction rate (mol m^{-3}_{cat} s^{-1})
r_{PROP}	propylene formation rate (mol s^{-1} g^{-1})
SEM	scanning electron microscopy
STP	standard temperature and pressure
T_b	bulk temperature (K)
TPD	temperature programed desorption
W	catalysts weight (g)
W/F_{0EtOH}	ethanol space time (g s μmol^{-1})
W/F_{0IPA}	isopropanol space time (g s μmol^{-1})
W/F_{0MeOH}	methanol space time (g s μmol^{-1})
X	conversion

Greek symbols

βe	external relative maximum temperature difference
βi	internal relative maximum temperature difference
ϕ	Thiele modulus
γ	Arrhenius number
η	effectiveness factor
λ_{eff}	thermal conductivity of the solid (J s^{-1} m^{-2} K^{-1})

1. Introduction

Lignocellulosic biomass based biorefineries can be considered as one of the most important future source for bioalcohols production, due to its great availability and limited price [1,2]. Among them, ethanol highlights due to their well-known use as biofuel. However, bioethanol production seems to exceed its consumption as fuel, and, therefore, there is room for its use as a platform molecule for the production of chemicals [3]. In this context, alcohols decomposition by dehydrogenation or dehydration is an important process for the production of different compounds of high interest for pharmaceutical and chemical industries [4].

Alcohol decomposition has been studied on a large variety of catalysts, as materials based on noble metals [5], oxides of transition metals [6], zeolites [7,8], silicoaluminophosphates [9], heteropolyacids [10], activated carbons [11,12] and sulfated zirconia [13] among others. The porosity and, specially, the surface chemistry (i.e. presence of base or acid functionalities) are the responsible for the activity and selectivity of the catalyst.

These catalysts are mainly used in powder morphology. However, the use of low size fibers as catalyst can avoid problems arising from the mass transfer, which is essential when optimizing the reaction conditions. Typically, the diffusion problems are solved using smaller particle size, which leads to larger pressure drops and low porosity of the bed. In this sense, fibers as catalyst are easy to handle, may be packed or constructed in the best form to fit the particular use, show very small resistance to diffusion and produce lower pressure drop [14].

Carbon-based materials such as activated carbon fibers (ACFs) have gained considerable interest due to their large specific surface areas, easily functionalization and high chemical and thermal stability under severe conditions [15]. These properties

open their applicability for separation applications, energy storage and even as catalyst support [16–18]. Specifically, ACFs have been used as support for different catalysts [19,20], but only a few works are related to their use as catalysts by themselves.

Carbon fibers are typically derived from conventional fossil precursors (PAN and pitches). However, the increase of their demand, their high production cost, and their non-renewable origin make necessary the search for others low-cost, more sustainable and abundant precursors. With this regard, lignin highlights as renewable precursor. Large scale production of lignin is mainly associated to pulp and paper industry and bioethanol production in wood-to-ethanol biorefineries as by-product. However, only around 40% of the generated lignin is needed to cover the internal energy demand of a biorefinery. Co-production of high-value biobased products in biorefineries would be a promising option for optimized utilization of biomass. The use of lignin to obtain ACFs could also reduce their cost and can be also an interesting alternative to extend the life cycle of this industrial byproduct by the obtaining of high added-value materials [21–23].

In previous works, we proposed the use of electrospinning for the preparation of carbon fibers from lignin [24–27]. This simple and versatile technique allowed an accurate control of the morphology and composition of the fibers. It even provided the possibility of obtaining heteroatom-doped or metal loaded carbon fibers in a simple stage, only by adding the corresponding compound to the lignin solution [24,28,29].

In this work, Alcell lignin was used for the preparation of carbon fibers by electrospinning. The influence of H_3PO_4 concentration in the solution to be electrospun and the following carbonization temperature were studied in order to obtain different carbon fibers catalyst with a variety of porosity and surface chemistry. These ACFs were subsequently used as catalyst for alcohol decomposition reactions.

2. Materials and methods

2.1. Preparation of carbon fibers catalyst

Carbon fibers catalysts are prepared by electrospinning technique by using a coaxial configuration, being Alcell lignin used as raw material for the preparation of the carbon fibers. Phosphorus-containing lignin fibers are obtained by one-pot method using two different H_3PO_4/lignin ratios. The solution is prepared by mixing H_3PO_4/lignin/ethanol with a weight ratio of 0.1/1/1 and 0.3/1/1. All solutions are stirred overnight at 200 rpm and 60 ºC before electrospinning. In the case of the fibers prepared with the lowest amount of H_3PO_4 (0.1/1/1), a flow rate of 1 mL h^{-1} is pumped through the inner needle and 0.1 mL h^{-1} of ethanol (used as solvent) is pumped through the external one. For phosphorus-containing lignin fibers with a H_3PO_4/lignin weight ratio of 0.3, a flow rate of 3 mL h^{-1} and 0.3 mL h^{-1} is needed through the internal and external needle, respectively.

The applied electric potential difference is 14 kV (collector potential at -7 kV and the tips at +7 kV) for phosphorus-containing lignin fibers with the lowest H_3PO_4/lignin ratio and 22 kV (collector at -11 kV and tip at +11 kV), for the production of phosphorus containing lignin fibers with the highest H_3PO_4/lignin ratio. The tip-to-collector distance is 25 cm in both cases.

Phosphorus-containing lignin fibers are stabilized under air atmosphere using a flow rate of 50 cm^3(STP) min^{-1}. The stabilization is carried out from room temperature to 200 ºC, at a heating rate of 0.8 ºC min^{-1} and the final temperature is kept for 1 h. As previously reported, the incorporation of H_3PO_4 to the initial lignin/ethanol solutions allows a faster fiber stabilization [29].

Stabilized fibers are carbonized in a tubular furnace at 500 ºC and 900 ºC under a continuous flow of N_2 (150 cm^3(STP) min^{-1}) with a heating rate of 10 ºC min^{-1}. After

that, carbonized fibers are washed with distilled water at 60 ºC. The carbon fibers prepared at 900 ºC are also thermally treated at 1200 and 1600 ºC. The nomenclature used in this work is the acronym PCF for the phosphorus-containing carbon fibers, followed by L for the lowest H_3PO_4/lignin mass ratio (0.1/1/1) used and H for the highest one (0.3), respectively. The final preparation temperatures are also included at the end of the name. For example, the sample PCFH1200 refers to a phosphorus-containing carbon fiber with an H_3PO_4/lignin ratio of 0.3, obtained at 900 ºC and followed by a thermal treatment at 1200 ºC.

2.2. Characterization of carbon fibers catalyst

The surface area and porosity of the carbon fibers are characterized by N_2 adsorption-desorption at -196 ºC, and by CO_2 adsorption at 0 ºC performed in a Micromeritics ASAP 2020 apparatus. Samples are outgassed at 150 ºC temperature for at least 8 h. From the N_2 isotherm, the apparent surface area (A_{BET}) is determined by applying the Brunauer Emmet and Teller equation [30]. From the CO_2 adsorption data, the narrow micropore surface area (A_{DR}) is calculated using the Dubinin-Radushkevich equation [31].

The size, shape and texture of the carbon fibers are analyzed by scanning electron microscopy (SEM) in a JSM 6490LV JEOL instrument. The surface chemistry of the sample is analyzed by X-ray photoelectron spectroscopy (5700C model Physical Electronics) with Mg kα radiation (1253.6 eV). Temperature-programmed desorption (TPD) is usually used to characterize the oxygen functional groups present in the carbon surface, which are formed during carbonization/activation processes. TPD analyses are obtained in a customized quartz fixed-bed reactor placed inside an electrical furnace and coupled to a mass spectrometer (Pfeiffer Omnistar GSD-301) and to non-dispersive

infrared (NDIR) gas analyzers (Siemens ULTRAMAT 22) in order to quantify CO and CO_2, (calibration error < 1%). In these experiments, c.a. 50 mg of the carbon fibers are heated from room temperature to 930 °C at a heating rate of 10 °C min^{-1} in nitrogen (purity 99.999%) flow (200 cm^3(STP) min^{-1}).

The total acidity of the catalyst prepared with H_3PO_4 is determined by chemisorbed pyridine at 120 ºC in a CI Electronics MK2 balance. The analysis is performed using about 15 mg of catalyst. The inlet partial pressure of pyridine was 0.02 atm. After saturation of the carbon fibers catalyst, desorption of physisorbed pyridine is carried out at the adsorption temperature in nitrogen flow.

The thermal stability of the catalysts in an oxidative atmosphere was studied by non-isothermal thermogravimetric analyses in a CI Electronics MK2 balance under air flow (150 cm^3 min^{-1}) from room temperature to 900 ºC at a heating rate of 10 ºC min^{-1}.

2.3. Alcohol decomposition experiments

The catalytic activity of the carbon fibers is studied by decomposition of different alcohols in the gas phase at atmospheric pressure in a fixed bed microreactor (i.d. 4 mm) placed inside a vertical furnace with temperature control, under different operating conditions. In a typical experiment 60 mg of catalyst are used. Alcohol is fed to the system in a controlled way by using a syringe pump (Cole-Parmer® 74900-00-05 model). Alcohol decomposition reaction is carried out in inert or oxidizing atmosphere in the temperature range of 200-700 ºC (depending on the carbon fibers to obtain a conversion of 100 %). To avoid condensation of any compound, all the lines are heated up to 120 ºC. Alcohol partial pressures from 0.01 to 0.08 atm (in N_2 or air) and space times between 0.02 and 0.1 g s μmol^{-1} are used for the different alcohol decomposition experiments.

The reactants and products concentrations in the outlet gas stream are analyzed by gas chromatography (490 micro-GC equipped with PPQ, MolSieve 5A and Wax columns, Agilent). The conversion is defined as the molar ratio of alcohol converted to alcohol fed to the reactor. The selectivity is defined as the molar concentration of a given product to that of the total products formed. The carbon balance is reached, in all the experiments, with an error lower than 5%.

3. Results and Discussion

3.1. Characterization of carbon fibers catalysts

Figure 1 shows SEM micrographs of the different phosphorus-containing carbon fibers catalysts. The mats obtained with this technique consisted of randomly oriented carbon microfibers, with fiber diameters ranging from 0.5 to 4 μm. The average diameter and size distribution of the fibers become wider as the phosphoric acid concentration in the lignin solution increases as a consequence of the higher electrical potential applied in this case. The morphology of the fibers is not modified after the carbonization step, confirming the successful thermostabilization of the lignin fibers. Meanwhile, the average size of the carbonized fibers decreases due mainly to the dehydration, condensation and dehydrogenation reactions that take part in the carbonization of lignin, associated to an important mass loss [32]. The smaller diameters are achieved at the highest preparation temperature related with a higher aromatization and dehydrogenation of carbon fibers structure. Finally, the Energy Dispersive X-Ray (EDX) mapping analysis of PCFH900 evidence a uniform distribution of carbon, oxygen and phosphorus in carbonized fibers, Figure 1i.

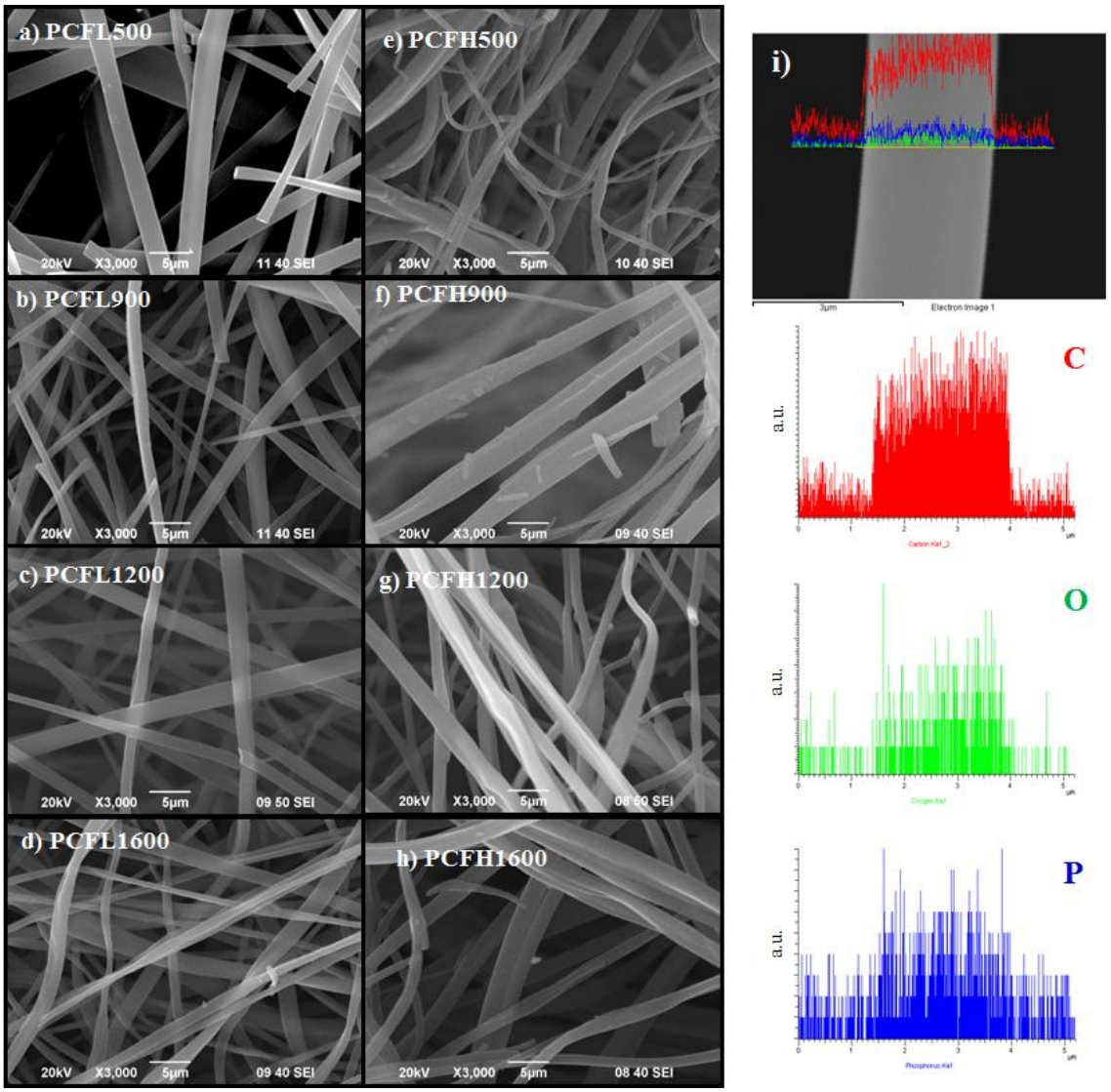

Figure 1. SEM micrographs of phosphorus-containing carbon fibers catalysts prepared at different temperatures. a-d) PCFLs, e-h) PCFHs, i) element distribution by EDX analysis of PCFH900.

Figure 2 collects the apparent surface area (A_{BET}) derived from the N_2 adsorption-desorption isotherms at -196 ºC (a) as well as the narrow micropore surface area (A_{DR}) obtained from the CO_2 adsorption isotherms at 0 ºC (b) as a function of the preparation temperature for all the carbon fibers. The carbonization of the lignin fibers produces the development of microporosity, as depicted by the high values of apparent surface area (values ranging from 400 to 1100 $m^2\ g^{-1}$) observed for all the samples. In addition, the

A_{BET}/A_{DR} ratios are close to one, suggesting the presence of narrow microporosity (average pore size of 0.5-0.7 nm) [33]. The values of external surface area, which are related to the presence of mesoporosity, are very low (< 15 m^2 g^{-1}) for all the samples, also evidencing the predominance of microporosity in these carbon fibers.

As can be seen in Figure 2, the maximum values of surface area for all the phosphorus-containing carbon fibers are produced when the samples are carbonized at 900 ºC. From this temperature, and due to the porosity shrinkage, a decrease of around 30% of A_{BET} is observed after the thermal treatment at 1600 ºC, independently of the amount of phosphoric acid incorporated in the preparation of the fibers. It is important to highlight that in spite of the high preparation temperature used, the carbon fibers present a high development of the porosity even at 1600 ºC, with apparent surface area values of approximately 650 and 830 m^2 g^{-1}, for PCFL1600 and PCFH1600 samples, respectively. The surface area values herein reported are between the largest reported in the literature for carbon fibers derived from lignin [24,34], and they were obtained without implementing further activation steps on the carbonized fibers.

Furthermore, the higher the H_3PO_4/lignin ratio is, the higher the apparent surface area is produced, with values ranging from 750 to 1150 m^2 g^{-1} for the highest amount of H_3PO_4 used, as a consequence of the well-known activating effect of the phosphoric acid. In this sense, the increase in the relative amount of phosphoric acid generates a higher development of porosity [35].

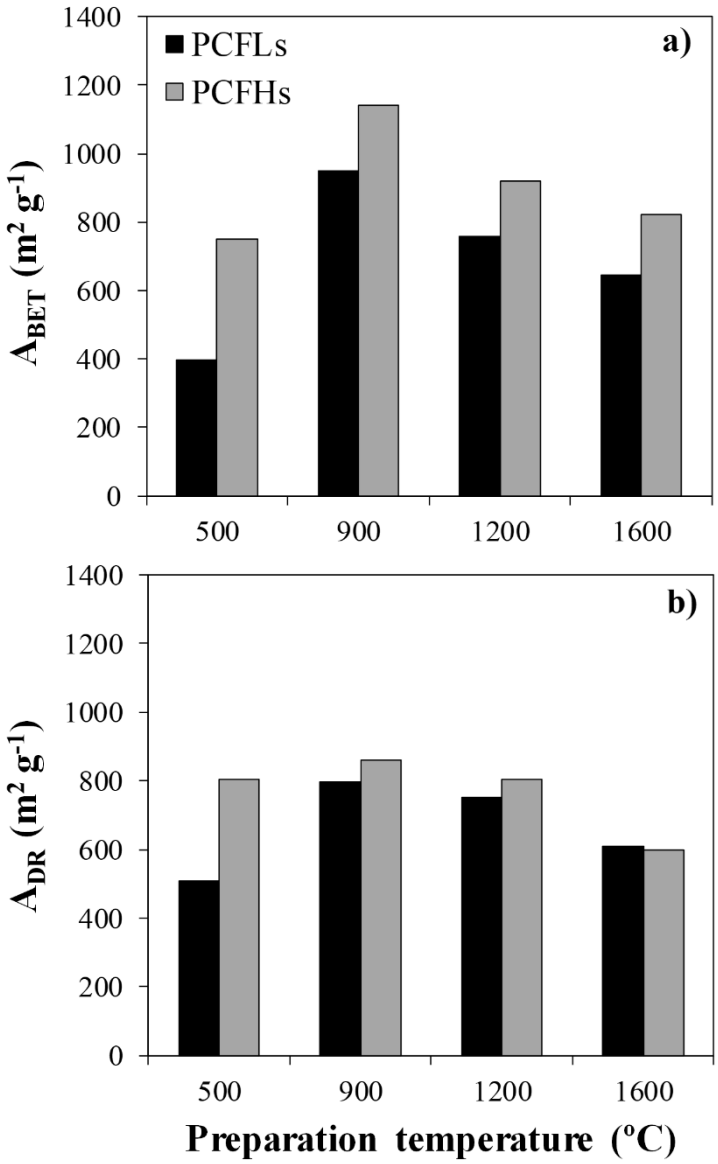

Figure 2. Surface area values derived from N_2 adsorption-desorption isotherms at -196 ºC (a) and from CO_2 adsorption isotherms at 0 ºC (b) of phosphorus-containing carbon fibers as a function of the preparation temperature.

Figure 3 shows the chemical surface composition of the phosphorus-containing carbon fibers analyzed by XPS. Carbon content increases with the preparation temperature, meanwhile the oxygen concentration decreases, for both impregnation ratios. In general,

carbon content values increase with the impregnation ratio for all the evaluated temperatures.

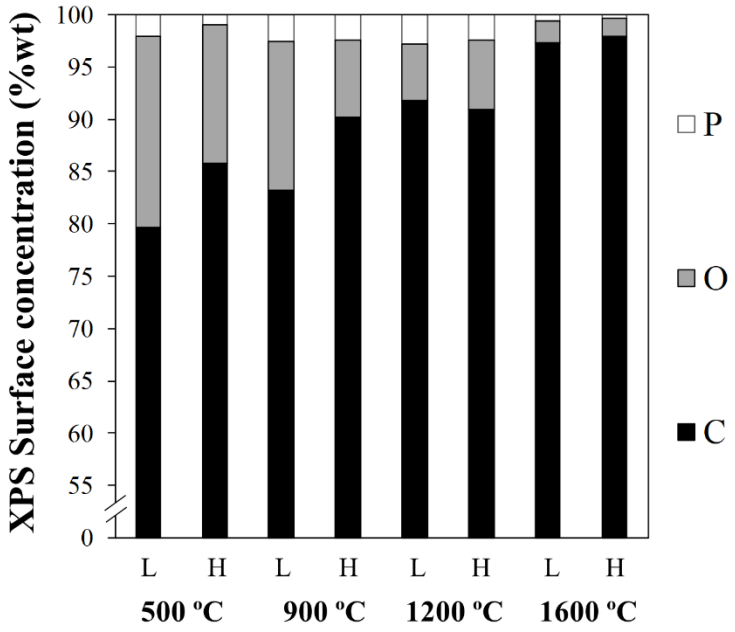

Figure 3. Chemical surface composition derived from XPS quantitative analyses of the different phosphorus-containing carbon fibers as a function of the preparation temperature.

The samples also show some phosphorus content, derived from the preparation method, but this phosphorus remains stably bonded to the carbon surface even after the washing step [35,36]. The values of phosphorus contents are lower than 3% wt. for all the carbon fibers, presenting a maximum value at 1200 ºC for both H_3PO_4/lignin ratios, what evidences the high stability of these phosphorus complexes on the carbon surface. From this temperature, these values decrease to contents lower than 0.6% due to the reduction of the phosphorus groups by the carbon and the subsequent volatilization of elemental P.

TPD is used to characterize the oxygen functional groups formed, in the carbon surface, during carbonization/activation processes. Table 1 presents the CO and CO_2 evolved

amounts during TPD experiments for all the carbon fibers catalysts. According to literature, carbon-oxygen groups of acidic character, such as carboxylic and lactonic, evolve as CO_2 upon thermal decomposition, whereas non-acidic, such as carbonyl, ether, quinone and phenol, evolve as CO. Anhydride surface groups evolve as both CO and CO_2 [37]. In this sense, carbon-oxygen groups of acidic character could be very interesting for alcohol dehydration reactions [38], but the amount of these groups is much lower than that of CO-evolving groups in all the samples. For both H_3PO_4/lignin mass ratios, CO_2/CO ratios of ca. 0.2 are observed at preparation temperatures of 500 and 1200 ºC, while a value slightly lower than 0.1 being reached at 900 ºC. Moreover, the amount of CO released during the TPD of the samples carbonized at 500 and 900 ºC are in line with those observed for activated carbons obtained by H_3PO_4 activation of lignocellulosic wastes [35,39,40], and also larger than those recorded for lignin-based electrospun carbon fibers [27]. We have previously reported that the CO evolution observed in H_3PO_4-activated carbons at temperatures on the 700 to 900 ºC range are the result of the thermal decomposition of the C-O-P bonds from phosphorus surface groups [41], which are also probably formed in the surface of PCFL and PCFH samples. Furthermore, the amount of oxygen surface groups evolving both as CO and CO_2 decreases with the preparation temperature, and this reduction is specially accused from 1200 ºC. This agrees with the XPS results, where a large decline in the amount of oxygen and phosphorus groups as the preparation temperature increases is observed, Figure 3.

The acidity of the carbon fibers is evaluated by pyridine chemisorption, whose chemisorbed amounts are also collected in Table 1. Pyridine was selected because it is able to characterize both Lewis and Brönsted acidic sites, although the preparation of carbon materials by chemical activation of H_3PO_4 is going to provide preferentially

Brönsted acidic sites [42]. In this sense, the amounts reported in this table are in the same range than the values reported for powder activated carbons obtained by chemical activation with phosphoric acid at ten times higher impregnation ratios, what seems to indicate the relevant acidity of the carbon fibers [43]. In addition, the amount of chemisorbed pyridine keeps a clear relationship with the phosphorus content of the carbon fibers determined by XPS analyses, showing a maximum for the carbon fibers prepared at 1200 ºC. In line with this, the amount of pyridine chemisorbed pyridine per P content (calculated as mol of pyridine chemisorbed per mol of phosphorus content determined by XPS) is much higher in these carbon fibers (1.83 mol Py mol^{-1} P for PCFH1200) than in other acid activated carbon catalysts with higher P content (0.48 mol Py mol^{-1} P) [44], suggesting the larger availability of acid functional groups on activated carbon microfibers owing to their improved mass transfer rate [14].

Table 1. CO and CO_2 evolved amounts from TPD experiments and pyridine chemisorbed values.

Carbon catalyst	**TPD (mmol g^{-1})**		**Pyridine chemisorbed (mmol g^{-1})**
	CO	**CO_2**	
PCFL500	2.74	0.58	1.22
PCFL900	2.43	0.23	1.59
PCFL1200	1.43	0.31	1.69
PCFL1600	0.21	0.08	0.86
PCFH500	2.33	0.53	1.48
PCFH900	4.40	0.40	1.49
PCFH1200	1.10	0.23	1.81
PCFH1600	0.24	0.08	0.96

Carbon materials with high oxidation resistance are necessary for allowing their use as catalysts and/or catalyst supports in several reactions under oxidizing conditions

[45,46]. In particular, the presence of O_2 in the reaction atmosphere is generally required to enhance the catalytic conversions, to avoid the possible deactivation and to reach steady-state conditions [44,47]. With this regard, the loss weight profiles under air atmosphere of the different phosphorus-containing carbon fibers are shown in Figure 4. As can be seen, phosphorus-containing carbon fibers catalysts present relatively high oxidation resistance, starting to oxidize at temperatures higher than 450 ºC. In previous works, the oxidation resistance of activated carbons prepared by chemical activation with phosphoric acid but at lower preparation temperatures was analyzed and their good performance under oxidizing conditions was related to the presence of the phosphorus groups on the carbon surface, which could act as a physical barrier and/or block the active carbon sites for the oxidation reaction [46,47]. Specifically, oxidation of the most reduced phosphorus groups, C-P, to most oxygenated phosphorus groups, mainly as C-O-PO_3 was suggested to be taken place, avoiding the carbon oxidation and thus retarding the gasification of the carbon matrix.

The increase in the preparation temperature (carbonized fibers treated at 1200 and 1600 ºC) produces carbon fibers with very high oxidation resistance, starting to gasify at temperatures higher than 600 ºC, in spite of the high apparent surface area of these catalysts. These results can be associated to the further increase of the structural ordering of the carbon fibers, and to the loss of superficial defects [48].

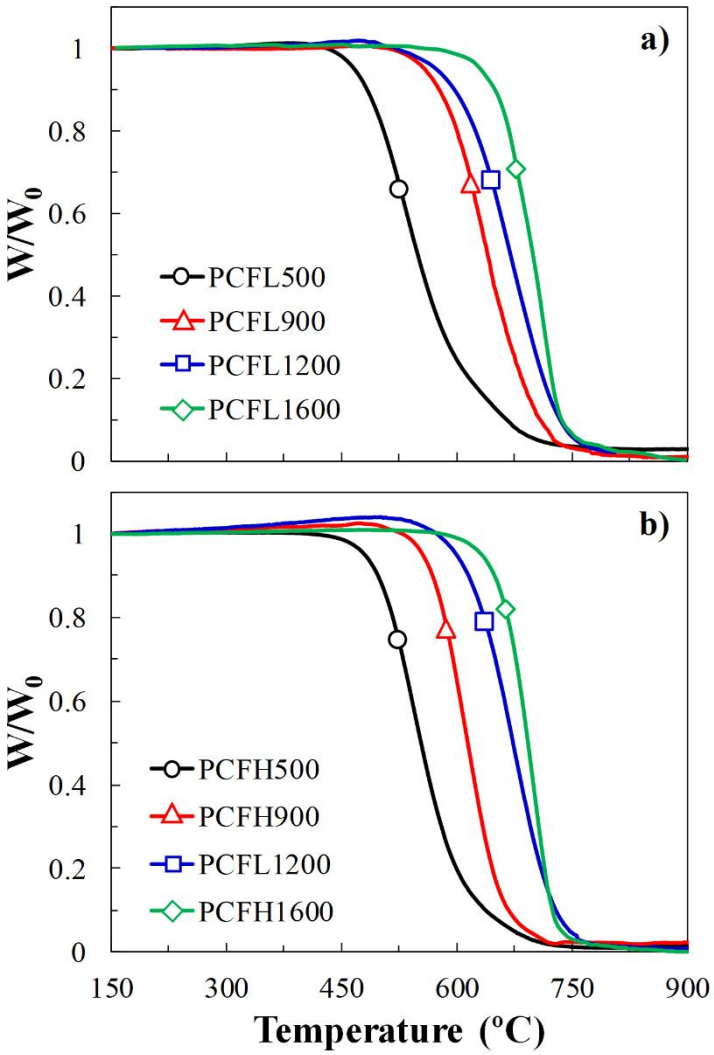

Figure 4. Non isothermal loss weight profiles of the different phosphorus containing carbon catalysts: a) PCFL and b) PCFH carbon series, respectively.

3.2. Isopropanol decomposition

3.2.1. Mass and heat transfer limitations calculation

The possible occurrence of external and internal mass and heat transfer limitations for the carbon fibers catalysts was elucidated using the corresponding dimensionless numbers [49]. For the external mass-transfer limitations, the Carberry number (*Ca*) was calculated by using equation (1).

$$Ca = \frac{r_{obs}}{r_{max}} = \frac{r_{obs}}{k_g \cdot a' \cdot C_b} \qquad (1)$$

where r_{obs} is the reaction rate (mol m^{-3}_{cat} s^{-1}) and r_{max} is the maximum mass transfer rate (mol m^{-3}_{cat} s^{-1}), which can be calculated by equation (2):

$$r_{max=}\, k_g \cdot a' \cdot C_b \qquad (2)$$

here, k_g represents the mass transfer coefficient (m s^{-1}), *a'* is the specific area and it is related to the ratio between particle surface area and particle volume (m^2 m^{-3}) and C_b is the bulk concentration (mol m^{-3}).

For the internal mass-transfer limitations, Thiele modulus (ϕ) and effectiveness factor (η) were analyzed. Equation (3) was used for the calculation of the Thiele modulus:

$$\phi = R_f \sqrt{\frac{k_v}{D_{eff}}} \qquad (3)$$

where R_f refers to the carbon fiber radius (m), k_v is the isopropanol rate constant (s^{-1}) assuming first order kinetics and D_{eff} (m^2 s^{-1}) is the effective diffusion coefficient.

The effectiveness factor was determined as a function of Thiele modulus by equation (4):

$$\eta = \frac{tanh\phi}{\phi} \qquad (4)$$

Moulinjn et at. proposed a criterion to evaluate the internal and extrernal heat transfer limitations in the catalysts. In order to avoid external heat transfer limitations, equation (5) has to be fulfilled:

$$\bar{\beta}_e \cdot \gamma \cdot Ca < 0.05 \qquad (5)$$

$$\bar{\beta}_e = \frac{\Delta T_{max}}{T_b} = \frac{k_g \cdot C_b \cdot (-\Delta H_r)}{h \cdot T_b} \qquad (6)$$

$$\gamma = E_a/R \cdot T_b \qquad (7)$$

being $\bar{\beta}_e$ the external relative maximum temperature difference, ΔH_r the reaction enthalpy (J mol^{-1}), *h* the heat transfer coefficient in the gas phase (J s^{-1}·m^{-2} K^{-1}), T_b the bulk temperature (K), E_a the activation energy of the reaction (J mol^{-1}) and γ the Arrhenius number. For the calculation of internal heat transfer limitations, the following equation was used:

$$\bar{\beta}_i \cdot \gamma \cdot (\eta \cdot \phi^2) < 0.05 \quad (8)$$

$$\bar{\beta}_i = \frac{\Delta T_{max}}{T_b} = \frac{D_{eff} \cdot C_s \cdot (-\Delta H_r)}{\lambda_{eff,p} \cdot T_b} \quad (9)$$

Where $\bar{\beta}_i$ is the internal relative maximum temperature difference and $\lambda_{eff,p}$ is the thermal conductivity of the solid (J s^{-1} m^{-2} K^{-1}).

The dimensionless numbers obtained after the calculation of mass and heat transfer limitations are summarized in Table 2. *Ca* values lower than 10^{-6} were obtained for all range of diameters and bed porosity values, evidencing the absence of external mass transfer limitations (valid for *Ca*<0.05). Effectiveness factor higher than 0.998 and Thiele Modulus lower than 0.072 were obtained for all the carbon fibers diameters and bed porosities ranges used, suggesting the absence of internal mass transfer limitations. In all the experimental conditions evaluated, values of $\bar{\beta}_e \cdot \gamma \cdot Ca$ and $\bar{\beta}_i \cdot \gamma \cdot (\eta \cdot \phi^2)$ were lower than 10^{-7}, indicating the absence of external or internal heat transfer limitations.

Table 2. Dimensionless number for internal and external mass and heat transfer limitation for isopropanol decomposition under inert and oxidizing atmosphere.

Carbon fibers catalysts	**Mass transfer**			**Heat transfer**	
	External limitations	External limitations		External limitations	External limitations
	Ca	**ϕ**	**η**	$\bar{\beta}_e \cdot \gamma \cdot Ca$	$\bar{\beta}_i \cdot \gamma \cdot (\eta \cdot \phi^2)$
N_2 atmosphere					
PCFL500	3.0 10^{-7}	0.0301	0.9997	5.9 10^{-8}	9.8 10^{-8}
PCFL900	1.1 10^{-7}	0.0204	0.9999	2.3 10^{-8}	4.8 10^{-8}
PCFL1200	4.8 10^{-8}	0.0421	0.9994	1.3 10^{-8}	2.7 10^{-7}
PCFL1600	2.7 10^{-8}	0.0012	1.0000	4.5 10^{-9}	1.3 10^{-10}
PCFH500	3.0 10^{-7}	0.0240	0.9998	6.6 10^{-8}	7.0 10^{-8}
PCFH900	1.9 10^{-7}	0.0129	0.9999	4.4 10^{-8}	2.1 10^{-8}
PCFH1200	1.9 10^{-7}	0.0535	0.9990	6.1 10^{-8}	4.9 10^{-7}
PCFH1600	1.9 10^{-7}	0.0102	1.0000	3.0 10^{-8}	8.9 10^{-9}
Air atmosphere					
PCFH500	1.6 10^{-6}	0.0411	0.9994	6.8 10^{-8}	2.2 10^{-7}
PCFH900	1.0 10^{-6}	0.0648	0.9986	4.6 10^{-8}	5.7 10^{-7}
PCFH1200	1.0 10^{-6}	0.0735	0.9982	5.0 10^{-8}	8.1 10^{-7}
PCFH1600	1.0 10^{-6}	0.0386	0.9995	4.6 10^{-8}	2.0 10^{-7}

3.2.2. Performance of the catalysts

The pseudo-steady state conversions under inert atmosphere of isopropanol (IPA) and selectivity to propylene/diisopropyl ether as a function of the reaction temperature for the different phosphorus-containing carbon fibers catalysts are shown in Figure 5. For the sake of comparison, the conversions and selectivity of a commercial γ-Al_2O_3 and their corresponding values for the homogeneous reaction were also included.

As expected, a rise of the reaction temperature produces an increase of the isopropanol conversion for all the catalysts. The activity of these carbon fibers follows the sequence of preparation temperatures 1200 > 900 > 500 > 1600 ºC, respectively, which is directly related to the amount of P on the fiber surface (determined by XPS analyses), and also to the acidity values evaluated by pyridine chemisorption. By this way, the sample prepared at 1200 ºC, with higher P content and acidity, is the most active.

Samples prepared with the highest impregnation ratio (PCFH) show slightly larger conversions at the same reaction temperature, under inert atmosphere. Furthermore, the comparison of the phosphorus containing carbon catalysts prepared at 1200 ºC with the commercial acid catalyst γ-Al_2O_3 evidences the high activity of both catalysts, with only a difference of 20 ºC for obtaining the same conversion.

Furthermore, in the case of the phosphorus containing carbon fibers prepared at 500, 900 and 1200 ºC, isopropanol decomposition reaction yields only propylene for the entire range of reaction temperatures, excepting at the lowest conversions (X<15%, obtained at temperatures lower than 225 ºC), where the reaction also produces diisopropyl ether as co-product with yields lower than 3%. This is a consequence of the high acidity of these activated carbon fibers. In this line, other lignocellulosic residues were already activated with phosphoric acid and showed high activity for the alcohol dehydration reaction [42,50]. This high activity was associated to the presence of both

P–OH and C-O-P groups, derived from phosphates and polyphosphates esters formed during the activation step, which can act as Brönsted acid sites with relatively strong strength and moderate/low acidity, respectively [42,47,50].

The complete isopropanol conversion for carbon fiber catalysts prepared at 1600 ºC requires a further increase in the reaction temperature. In spite of the removal of almost all oxygen surface groups and the low P content of these fibers on the carbon surface (see Figure 3 and Table 1), the selectivity to propylene is still high (selectivity values over 90% up to 600 ºC), indicating the presence of some acidic character, probably related to the remaining P groups. Selectivity to diisopropyl ether increases at higher temperatures due to the contribution of the thermal decomposition of isopropanol in gas phase.

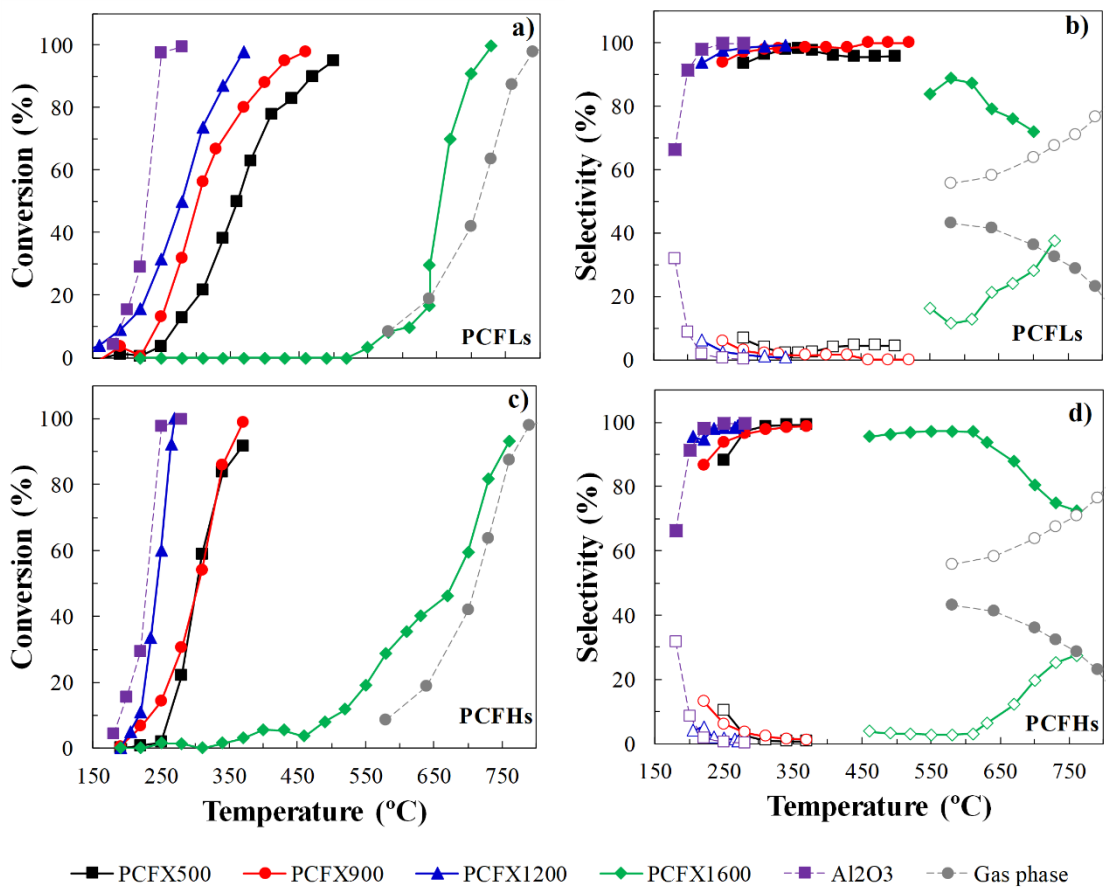

Figure 5. Steady state conversion of isopropanol for the different phosphorus-containing carbon fibers (a, c) and selectivity to propylene (filled symbols) and diisopropyl ether (hollow symbols) (b, d) as a function of the reaction temperature, under inert atmosphere. P_{0IPA}= 0.0185 atm; W/F_{0IPA}= 0.04 g s µmol^{-1}.

The influence of the presence of air in the isopropanol decomposition is also analyzed for the PCFH catalysts series in Figure 6. In general, the phosphorus-containing carbon fibers catalysts increase their activity in the presence of oxygen, especially at the lowest reaction temperatures (150-225 ºC). In addition, a change in the products distribution for all the carbon catalysts is observed, especially, at these low temperatures. As can be seen in Figure 6b, these catalysts still produce propylene, with selectivity values over 60% in all the cases, but also significant amounts of acetone, related to the oxidative dehydrogenation of isopropanol. The contribution of this reaction decreases with increasing the temperature.

The most relevant change in the presence of oxygen is related to the great shift to lower reaction temperatures of the conversion profile for the catalyst PCFH1600, Figure 6a. In this sense, an increase of the P content from 0.3 to 0.6% has been determined by XPS analyses on PCFH1600 after the reaction. These results suggest that only the most external phosphorus groups are reduced to P^0 and volatilized during the thermal treatment at 1600 ºC, while inner phosphorus groups that cannot be detected by XPS remains stably linked to the carbon surface. The treatment with oxygen seems to favor the migration of these phosphorus complexes to the external surface.

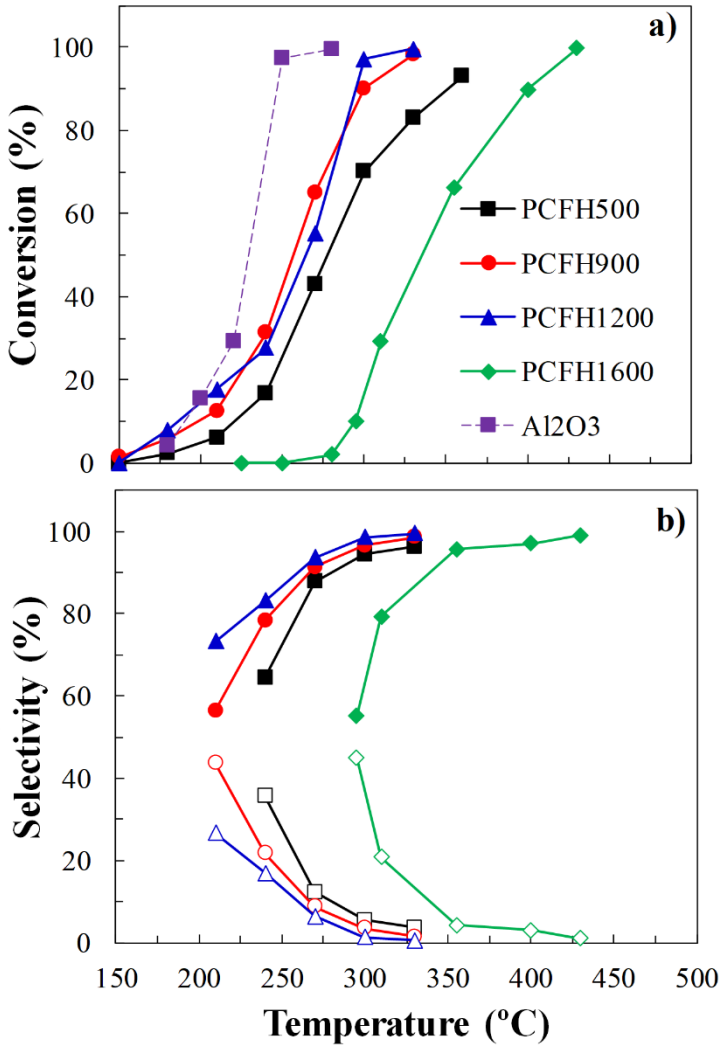

Figure 6. Steady state conversion of isopropanol for PCFHs carbon fibers (a) and selectivity to propylene (filled symbols) and acetone (hollow symbols) (b) as a function of the reaction temperature, under air atmosphere. P_{0IPA}= 0.0185 atm; W/F_{0IPA}= 0.04 g s µmol^{-1}.

3.2.3. Kinetic study

Apparent kinetic parameters were estimated from the conversion vs temperature profiles assuming first-order kinetic for isopropanol decomposition in a preliminary approximation:

$$ln\left(\frac{1}{1-X}\right) = k \cdot P_{0IPA} \cdot \frac{W}{F_{0IPA}} \quad (10)$$

In this equation, k is the apparent rate constant (μmol atm^{-1} g^{-1} s^{-1}), W is the catalyst weight (g), F_{0IPA} is the isopropanol molar flow rate (μmol s^{-1}), P_{0IPA} is the isopropanol partial pressure (atm) and X is the conversion. The values of the apparent kinetic parameters (k_0 is the preexponential factor and E_a is the activation energy) for all the carbon fibers catalysts are summarized in Table 3. Values of activation energy from 63 to 111 kJ mol^{-1} are obtained for the different catalysts. These values are in the same range than those previously obtained for carbon based acid catalysts prepared from biomass by phosphoric acid activation for the dehydration of isopropanol [42,50]. The catalyst with the lowest activation energy is that obtained at 1200 ºC. Besides, the activation energy decreases with the increase of the impregnation ratio for all the preparation temperatures, suggesting an increase of the strength of the acid sites of the PCFH series [51]. The presence of air in the inlet stream generates an additional decrease of the activation energy, possibly related to the coupling of the oxidative dehydrogenation reaction, which has a lower activation energy [52].

Table 3. Apparent kinetic parameters for isopropanol decomposition over the different carbon catalyst series under inert (PCFL and PCFH) and air atmosphere (PCFH).

Preparation temperature ºC	**PCFL**		**PCFH**		**PCFH-air**	
	E_a kJ mol^{-1}	**Ln(k_0)**	**E_a kJ mol^{-1}**	**Ln(k_0)**	**E_a kJ mol^{-1}**	**Ln(k_0)**
500	79	22.1	70	21.5	66	20.8
900	80	23.5	73	21.8	65	21.0
1200	78	29.4	77	31.0	63	21.4
1600	111	20.2	94	19.5	70	19.8

A more detailed kinetic study was carried out for the most active catalyst, PCFH1200 under inert (N_2) atmosphere. With this goal, evolution of isopropanol conversion with space time at different temperatures (for a constant isopropanol inlet partial pressure of P_{0IPA}= 0.0185 atm) and with inlet partial pressure of isopropanol at different temperatures (for a constant space time of W/F_{0IPA}= 0.04 g s µmol^{-1}) can be analyzed in Figure 7. The used kinetic model was that already proposed by Bedia et al. for powder catalysts prepared from hemp residues by chemical activation with phosphoric acid **[42]**. The prediction of the kinetic parameters was carried out assuming an integral reactor behavior, where the reaction rate could be represented as follow:

$$\frac{dX_{IPA}}{d\left(\frac{W}{F_{0IPA}}\right)} = -r_{IPA} \quad (11)$$

The kinetic rate equation is based on a Langmuir-Hinshellwood expression, assuming that the surface reaction takes place by a concerted E2 elimination mechanism. This E2 mechanism takes into account that the leaving group, OH, and the ß proton depart in a unique step. E1 mechanism, where the adsorbed carbocation is formed, and subsequently a ß hydrogen departs, obtaining the corresponding propylene into two steps, was also analyzed, but significantly higher residual errors were obtained. In addition, the kinetic model was also simplified by neglecting the intermolecular

dehydration to the ether, due to the total conversion to diisopropyl ether is, in all cases, lower than 5% for this catalyst. With these considerations, the global reaction rate can be written as follows, for the E2 reaction type:

$$-r_{IPA} = r_{PROP} = \frac{k_{PROP} \cdot K_{IPA}.P_{IPA}}{1 + K_{IPA}.P_{IPA} + K_{PROP}.P_{PROP}} \quad (12)$$

The activation energy of the formation of adsorbed propylene (k_{PROP}, rate determining step) and the corresponding adsorption enthalpy of propylene were fixed at the same values reported by Bedia et al. **[42]**. The optimization of the rest of kinetic parameters was carried out by minimizing the error function between the experimental and simulated steady-state conversions and the obtained values are summarized in Table 4.

Table 4. Optimized kinetic parameters for isopropanol decomposition with PCFH1200.

K_{0IPA} L mol^{-1}	ΔH_{IPA} kJ mol^{-1}	k_0 mol g^{-1} s^{-1}	Ea kJ mol^{-1}	K_{0PROP} L mol^{-1}	ΔH_{PROP} kJ mol^{-1}
0.335	-33.2	$5.4 \cdot 10^5$	98.5	1.561	-33.4

As can be seen in Figure 7, the conversion increases with isopropanol partial pressure, being this effect more accused at higher temperatures. Isopropanol conversions also increases with space time over the evaluated temperature range. In this sense, the kinetic model previously reported by Bedia et al. is able to reproduce fairly well the experimental results, using the same activation energy and adsorption enthalpy values.With regard to the preexponential factor of the kinetic constant, a decrease of the value can be observed with respect to those obtained by Bedia et al., probably related to the lower presence of active sites per unit of surface area or unit of mass of carbon fibers catalyst **[50]**.

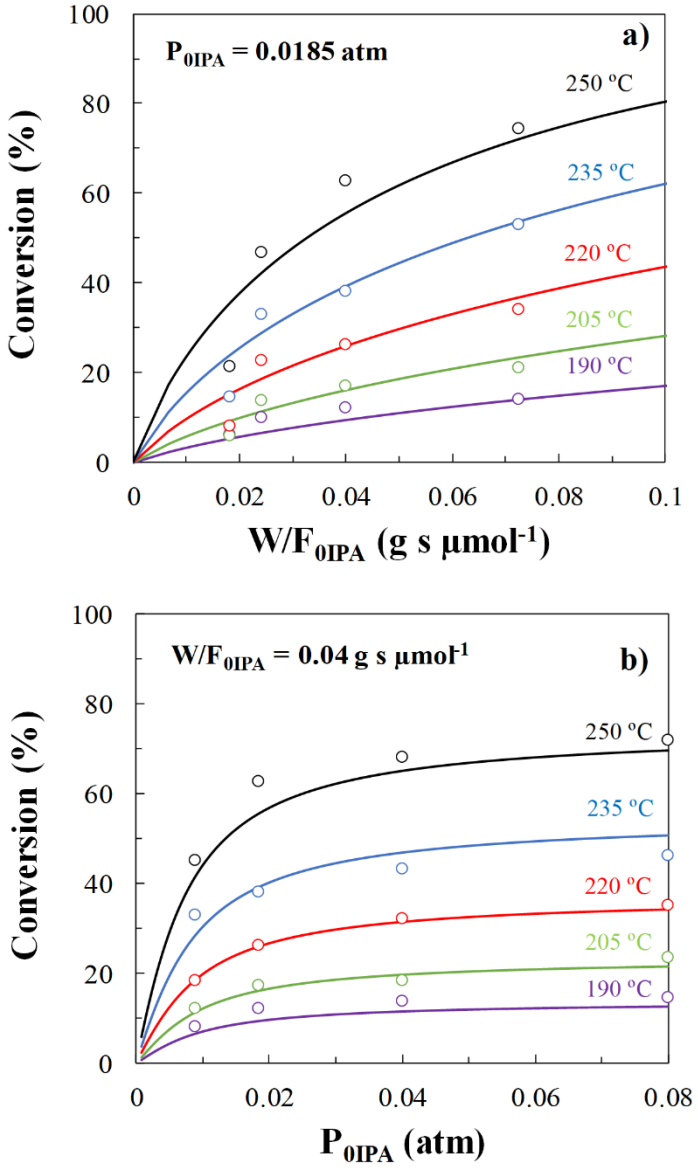

Figure 7. a) Evolution of isopropanol conversion with space time at different temperatures and constant isopropanol inlet partial pressure (P_{0IPA} = 0.0185 atm); b) evolution of isopropanol conversion with inlet partial pressure of isopropanol at different temperatures and constant space time (W/F_{0IPA} = 0.04 g s µmol $^{-1}$).

3.3. Ethanol and methanol decomposition

Ethanol and methanol decomposition reactions are also studied for the catalyst with the highest activity for isopropanol decomposition, PCFH1200. Figure 8 shows the conversion of ethanol (a) and methanol (b) as well as the selectivity to different

products as a function of the reaction temperature for this phosphorus-containing carbon catalyst under air atmosphere. As can be seen in Figure 8a the conversion of ethanol increases with the rising of the reaction temperature, showing ethanol conversion of 100% at 400 ºC. In the entire range of reaction temperatures evaluated, selectivity to ethylene remains higher than 80%, showing values higher than 90% for temperatures lower than 350 ºC. From this temperature, selectivity to diethyl ether begins to increase. These conversion values were comparable or even slightly higher than those recently reported in the literature for different catalysts, such as alumina and Al/SBA-15 **[53,54]**. Even though a few works report higher conversion or slightly higher selectivity at lower reaction temperatures, they use noble metals**[55]**, transition metals **[56,57]** as active phase, or they implied strong chemical treatments of zeolites **[58]**. When the conversion and selectivity of PCFH1200 is compared to other carbon-based catalysts, such as carbon-based catalyst from pyrolysis of waste tire **[59]** or heteropolyacids supported on activated carbons, this sample outperforms them. In contrast, the catalytic activity is slightly lower than the one determined for the activated carbon obtained from olive stone by chemical activation with phosphoric acid **[44]**. This last activated carbon presented twice the P content of PCFH1200, meaning that it probably has a larger amount of active sites, along with a wider microporosity (A_{BET}/A_{DR} ~ 2.4) and much larger external surface area (450 m^2 g^{-1}), which may facilitate the access to the active sites.

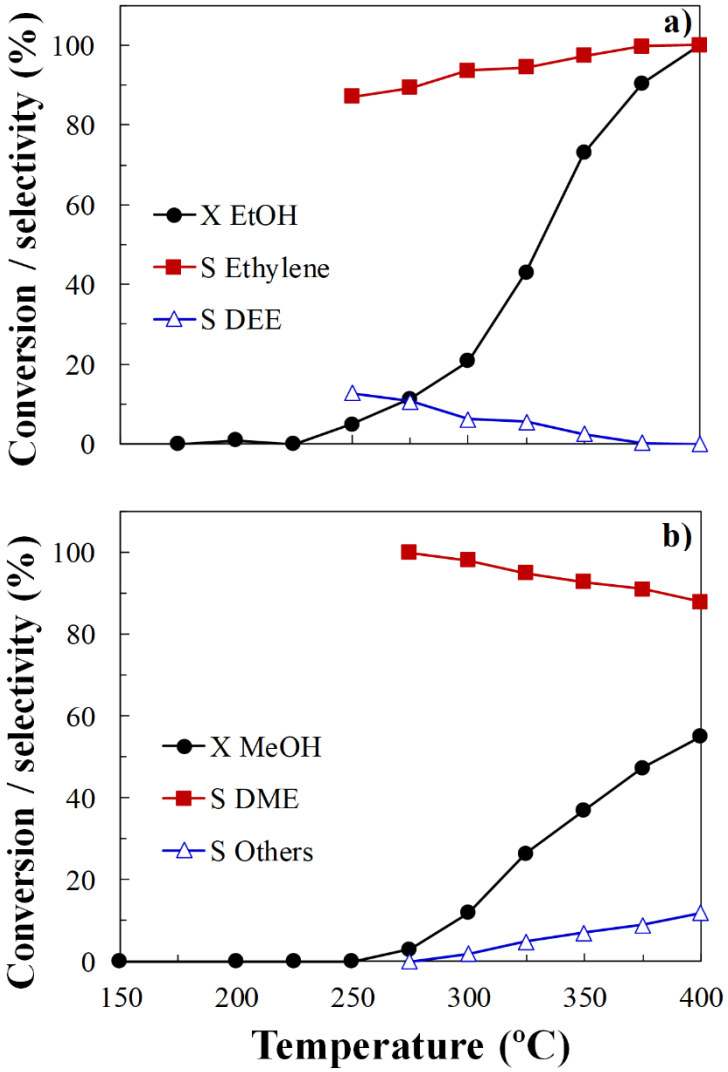

Figure 8. Conversion of ethanol (a) and methanol (b) and the corresponding selectivity to different products for the PCFH1200 carbon catalysts. $P_{0EtOH} = P_{0MeOH} = 0.02$ atm, $W/F_{0EtOH} = W/F_{0MeOH} = 0.1$ g s μmol $^{-1}$ under air atmosphere.

The production of DME, a promising alternative to Liquefied Petroleum Gas (LPG), by methanol dehydration is another potential application for acid catalysts. Thus, PCFH1200 was used as catalyst for the methanol dehydration in air atmosphere. Methanol conversion and selectivity values as function of the reaction temperature are collected in Figure 8b. In this case, methanol conversions

approximately of 60% are obtained at 400 ºC. The main reaction products are dimethyl-ether (DME) and CO/CO_2. The formation of the latter compound increases with the reaction temperature, but selectivity to DME higher than 90% is observed for all the reaction temperatures analyzed. At temperatures higher than 400 ºC and high time of stream (TOS) the gasification of the carbon fibers starts to be significant, what avoids their use as catalyst at those conditions. The values herein observed are very similar to those reported by Valero-Romero et al. with powder activated carbon obtained by chemical activation of olive stone with phosphoric acid **[47]**. It must be highlighted that the selectivity of this catalyst towards DME is higher than those reported for H-ZSM-5 zeolites, alumina and other inorganic catalysts **[60,61]**, although PCFH1200 is not able to reach the methanol conversions shown by them. In addition, the use of these carbon fibers presents the advantage of being obtained from a low-cost and renewable industrial byproduct (lignin) for the production of high added-value materials (fibrous catalysts).

Another relevant feature for carbon catalysts operating under strongly oxidizing atmospheres is their long-time stability. Figure 9 displays the ethanol and methanol conversions and selectivity of PCFH1200 catalyst at 325 ºC for long times of stream (TOS). The results clearly indicate that the conversion and selectivity for both ethanol and methanol dehydration are relatively high and steady at the selected operating conditions for the studied period of 12 h, with only a slight reduction of the ethylene formation with TOS (Figure 9a). These stability results can be associated to the spillover of oxygen by P-surface groups, what prevents these active surface sites from deactivation by carbonaceous deposits **[47]**.

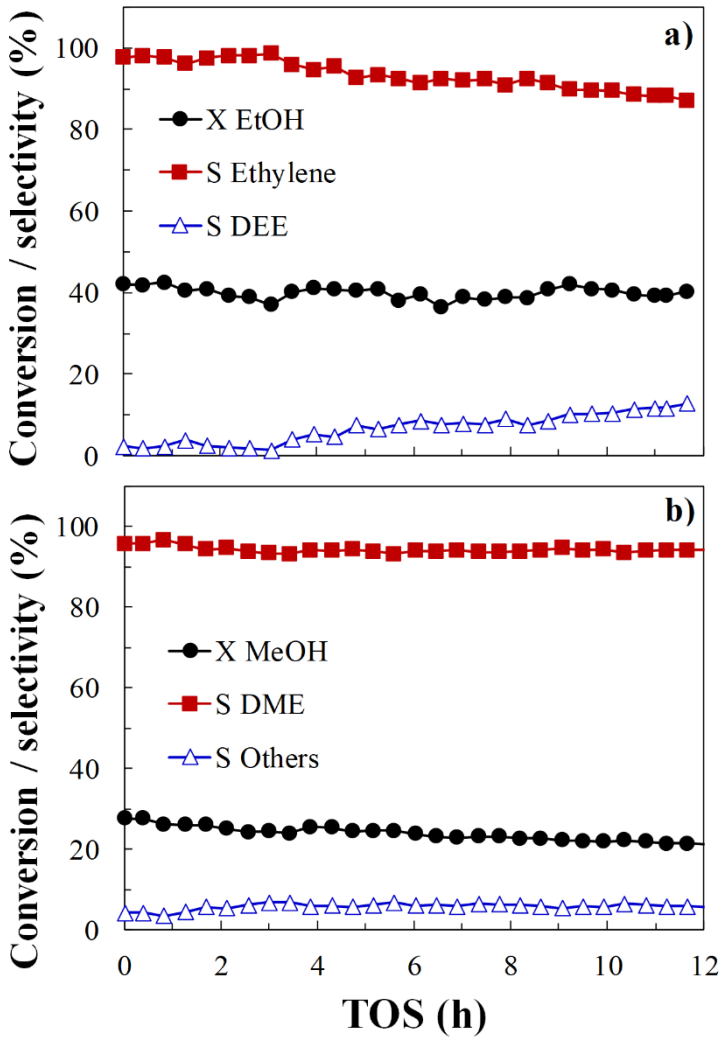

Figure 9. Evolution of ethanol (a) and methanol (b) conversion and selectivity as a function of time on stream at 325 ºC, for the PCFH1200 carbon catalysts. P_{0EtOH} = P_{0MeOH} =0.02 atm, W/F_{0EtOH} = W/F_{0MeOH} = 0.1 g s µmol $^{-1}$.

Bio-ethanol and bio-methanol streams are usually rich in water content, whose elimination is very costly. In this sense, the effect of the presence of water vapor on both ethanol and methanol conversion and selectivity is studied in order to evaluate the possibility of using these catalysts for the conversion of bio-alcohols. Figure 10 shows the ethanol and methanol steady state conversions for different inlet partial pressures of water at 350 ºC in air. In both cases, the alcohol conversions are only slightly decreased

in the presence of water; however, ethanol activity is more affected by the increase of the inlet partial pressures of water, showing a 30% decrease in conversion, which can be explained by the competitive adsorption between water and alcohol, being higher in the case of ethanol. In both cases, the selectivity towards dehydration remains unaffected.

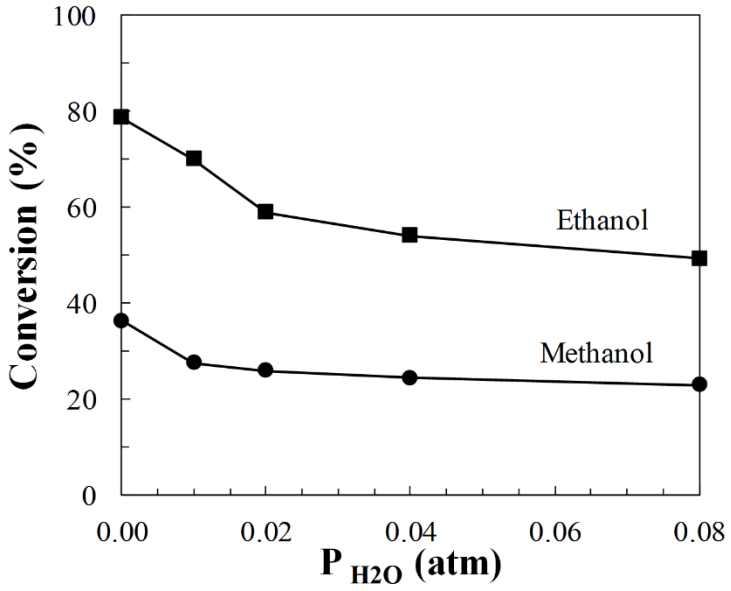

Figure 10. Ethanol and methanol conversions as a function of different partial pressures of water for PCFH1200 carbon catalysts. $P_{0EtOH} = P_{0MeOH} = 0.02$ atm, $W/F_{0EtOH} = W/F_{0MeOH} = 0.1$ g s μmol $^{-1}$ at 350 ºC.

4. Conclusions

Carbon fibers catalysts were prepared by electrospinning of Alcell lignin solutions. The use of H_3PO_4 in the initial lignin solution along with the variation of the carbonization temperature allowed the preparation of different carbon catalysts with a wide range of porosity and surface chemistry properties. Phosphorus-containing carbon fibers catalysts prepared with H_3PO_4 showed acid character. Thermal treatments at 1200 and 1600 ºC increased the oxidation resistance and provided some acidic character. These

acid carbon fibers catalysts showed high activity for the selective isopropanol conversion to propylene. The best performing carbon catalyst, PCFH1200, was only slightly less active for isopropanol decomposition under inert atmosphere than commercial γ-Al_2O_3 acid catalyst, with the advantages of being prepared in fibrillar morphology and from a low-cost and renewable industrial byproduct. The high oxidation resistance of the P-containing carbon fibers allowed using air in the reactor inlet stream, delivering higher reaction rates and increasing the acetone production via oxidative dehydrogenation and the propylene formation by dehydration.

Ethanol and methanol decomposition were also evaluated in air stream for the most active phosphorus-carbon catalyst, showing high conversion and selectivity to the dehydration product. These results suggest that phosphorus-containing carbon fibers prepared by electrospinning of lignin solutions seem to be excellent catalysts for alcohol decomposition reactions.

Acknowledgments

We gratefully thank MINECO (Project CTQ2015-68654-R) and MICINN (RTI2018-097555-B-100) for financial support. F.J.G.M. acknowledgments the assistance of MINECO for PTA2015-11464-I and Universidad de Málaga for postdoctoral contract.

References

[1] A.K. Mathew, A. Abraham, K.K. Mallapureddy, R.K. Sukumaran, Chapter 9 - Lignocellulosic Biorefinery Wastes, or Resources?, in: T. Bhaskar, A. Pandey, S.V. Mohan, D.-J. Lee, S.K. Khanal (Eds.), Waste Biorefinery, Elsevier, 2018: pp. 267–297. https://doi.org/10.1016/B978-0-444-63992-9.00009-4.

[2] M.C. Gutiérrez, J.M. Rosas, M.A. Rodríguez-Cano, I. López-Luque, J. Rodríguez-Mirasol, T. Cordero, Strategic situation, design and simulation of a biorefinery in Andalusia, Energy Convers. Manag. 182 (2019) 201–214. https://doi.org/10.1016/j.enconman.2018.12.038.

[3] J.M.R. Gallo, J.M.C. Bueno, U. Schuchardt, J.M.R. Gallo, J.M.C. Bueno, U. Schuchardt, Catalytic Transformations of Ethanol for Biorefineries, J. Braz. Chem. Soc. 25 (2014) 2229–2243. https://doi.org/10.5935/0103-5053.20140272.

[4] R.G. Grim, A.T. To, C.A. Farberow, J.E. Hensley, D.A. Ruddy, J.A. Schaidle, Growing the Bioeconomy through Catalysis: A Review of Recent Advancements in the Production of Fuels and Chemicals from Syngas-Derived Oxygenates, ACS Catal. 9 (2019) 4145–4172. https://doi.org/10.1021/acscatal.8b03945.
[5] M.L. Cubeiro, J.L.G. Fierro, Partial oxidation of methanol over supported palladium catalysts, Appl. Catal. Gen. 168 (1998) 307–322. https://doi.org/10.1016/S0926-860X(97)00361-X.
[6] N.E. Quaranta, J. Soria, V.C. Corberán, J.L.G. Fierro, Selective Oxidation of Ethanol to Acetaldehyde on V2O5/TiO2/SiO2Catalysts, J. Catal. 171 (1997) 1–13. https://doi.org/10.1006/jcat.1997.1760.
[7] F.S. Ramos, A.M.D. de Farias, L.E.P. Borges, J.L. Monteiro, M.A. Fraga, E.F. Sousa-Aguiar, L.G. Appel, Role of dehydration catalyst acid properties on one-step DME synthesis over physical mixtures, Catal. Today. 101 (2005) 39–44. https://doi.org/10.1016/j.cattod.2004.12.007.
[8] C.B. Phillips, R. Datta, Production of Ethylene from Hydrous Ethanol on H-ZSM-5 under Mild Conditions, Ind. Eng. Chem. Res. 36 (1997) 4466–4475. https://doi.org/10.1021/ie9702542.
[9] D. Chen, K. Moljord, A. Holmen, A methanol to olefins review: Diffusion, coke formation and deactivation on SAPO type catalysts, Microporous Mesoporous Mater. 164 (2012) 239–250. https://doi.org/10.1016/j.micromeso.2012.06.046.
[10] Y. Izumi, R. Hasebe, K. Urabe, Catalysis by heterogeneous supported heteropoly acid, J. Catal. 84 (1983) 402–409. https://doi.org/10.1016/0021-9517(83)90011-8.
[11] G.S. Szymański, G. Rychlicki, Importance of oxygen surface groups in catalytic dehydration and dehydrogenation of butan-2-ol promoted by carbon catalysts, Carbon. 29 (1991) 489–498. https://doi.org/10.1016/0008-6223(91)90112-V.
[12] C. Moreno-Castilla, F. Carrasco-Marín, C. Parejo-Pérez, M.V. López Ramón, Dehydration of methanol to dimethyl ether catalyzed by oxidized activated carbons with varying surface acidic character, Carbon. 39 (2001) 869–875. https://doi.org/10.1016/S0008-6223(00)00192-5.
[13] G.D. Yadav, J.J. Nair, Sulfated zirconia and its modified versions as promising catalysts for industrial processes, Microporous Mesoporous Mater. 33 (1999) 1–48. https://doi.org/10.1016/S1387-1811(99)00147-X.
[14] E. Reichelt, M. Jahn, Generalized correlations for mass transfer and pressure drop in fiber-based catalyst supports, Chem. Eng. J. 325 (2017) 655–664. https://doi.org/10.1016/j.cej.2017.05.119.
[15] M. Suzuki, Activated carbon fiber: Fundamentals and applications, Carbon. 32 (1994) 577–586. https://doi.org/10.1016/0008-6223(94)90075-2.
[16] C. Brasquet, P. Le Cloirec, Adsorption onto activated carbon fibers: Application to water and air treatments, Carbon. 35 (1997) 1307–1313. https://doi.org/10.1016/S0008-6223(97)00079-1.
[17] Y. Matatov-Meytal, M. Sheintuch, Catalytic fibers and cloths, Appl. Catal. Gen. 231 (2002) 1–16. https://doi.org/10.1016/S0926-860X(01)00963-2.
[18] Z. Chen, Y. Qin, D. Weng, Q. Xiao, Y. Peng, X. Wang, H. Li, F. Wei, Y. Lu, Design and Synthesis of Hierarchical Nanowire Composites for Electrochemical Energy Storage, Adv. Funct. Mater. 19 (2009) 3420–3426. https://doi.org/10.1002/adfm.200900971.
[19] I. Mochida, Y. Korai, M. Shirahama, S. Kawano, T. Hada, Y. Seo, M. Yoshikawa, A. Yasutake, Removal of SOx and NOx over activated carbon fibers, Carbon. 38 (2000) 227–239. https://doi.org/10.1016/S0008-6223(99)00179-7.

[20] H.T. Zheng, Y. Li, S. Chen, P.K. Shen, Effect of support on the activity of Pd electrocatalyst for ethanol oxidation, J. Power Sources. 163 (2006) 371–375. https://doi.org/10.1016/j.jpowsour.2006.09.062.
[21] J.M. Rosas, R. Berenguer, M.J. Valero-Romero, J. Rodríguez-Mirasol, T. Cordero, Preparation of different carbon materials by thermochemical conversion of lignin, Carbon-Based Mater. 1 (2014) 29. https://doi.org/10.3389/fmats.2014.00029.
[22] D.A. Baker, T.G. Rials, Recent advances in low-cost carbon fiber manufacture from lignin, J. Appl. Polym. Sci. 130 (2013) 713–728. https://doi.org/10.1002/app.39273.
[23] S. Chatterjee, T. Saito, Lignin-Derived Advanced Carbon Materials, ChemSusChem. 8 (2015) 3941–3958. https://doi.org/10.1002/cssc.201500692.
[24] F.J. García-Mateos, R. Ruiz-Rosas, J.M. Rosas, J. Rodríguez-Mirasol, T. Cordero, Controlling the Composition, Morphology, Porosity, and Surface Chemistry of Lignin-Based Electrospun Carbon Materials, Front. Mater. 6 (2019). https://doi.org/10.3389/fmats.2019.00114.
[25] M. Lallave, J. Bedia, R. Ruiz-Rosas, J. Rodríguez-Mirasol, T. Cordero, J.C. Otero, M. Marquez, A. Barrero, I.G. Loscertales, Filled and Hollow Carbon Nanofibers by Coaxial Electrospinning of Alcell Lignin without Binder Polymers, Adv. Mater. 19 (2007) 4292–4296. https://doi.org/10.1002/adma.200700963.
[26] R. Ruiz-Rosas, J. Bedia, M. Lallave, I.G. Loscertales, A. Barrero, J. Rodríguez-Mirasol, T. Cordero, The production of submicron diameter carbon fibers by the electrospinning of lignin, Carbon. 48 (2010) 696–705. https://doi.org/10.1016/j.carbon.2009.10.014.
[27] R. Berenguer, F.J. García-Mateos, R. Ruiz-Rosas, D. Cazorla-Amorós, E. Morallón, J. Rodríguez-Mirasol, T. Cordero, Biomass-derived binderless fibrous carbon electrodes for ultrafast energy storage, Green Chem. 18 (2016) 1506–1515. https://doi.org/10.1039/C5GC02409A.
[28] F.J. García-Mateos, T. Cordero-Lanzac, R. Berenguer, E. Morallón, D. Cazorla-Amorós, J. Rodríguez-Mirasol, T. Cordero, Lignin-derived Pt supported carbon (submicron)fiber electrocatalysts for alcohol electro-oxidation, Appl. Catal. B Environ. 211 (2017) 18–30. https://doi.org/10.1016/j.apcatb.2017.04.008.
[29] F.J. García-Mateos, R. Berenguer, M.J. Valero-Romero, J. Rodríguez-Mirasol, T. Cordero, Phosphorus functionalization for the rapid preparation of highly nanoporous submicron-diameter carbon fibers by electrospinning of lignin solutions, J. Mater. Chem. A. 6 (2018) 1219–1233. https://doi.org/10.1039/C7TA08788H.
[30] S. Brunauer, P.H. Emmett, E. Teller, Adsorption of Gases in Multimolecular Layers, J. Am. Chem. Soc. 60 (1938) 309–319. https://doi.org/10.1021/ja01269a023.
[31] M.M. Dubinin, E.D. Zaverina, Surface and sorption properties of active -carbons, Bull. Acad. Sci. USSR Div. Chem. Sci. 4 (1955) 531–538. https://doi.org/10.1007/BF01167331.
[32] J. Cao, G. Xiao, X. Xu, D. Shen, B. Jin, Study on carbonization of lignin by TG-FTIR and high-temperature carbonization reactor, Fuel Process. Technol. 106 (2013) 41–47. https://doi.org/10.1016/j.fuproc.2012.06.016.
[33] D. Lozano-Castelló, D. Cazorla-Amorós, A. Linares-Solano, Usefulness of CO2 adsorption at 273 K for the characterization of porous carbons, Carbon. 42 (2004) 1233–1242. https://doi.org/10.1016/j.carbon.2004.01.037.
[34] M. Kumar, M. Hietala, K. Oksman, Lignin-Based Electrospun Carbon Nanofibers, Front. Mater. 6 (2019). https://doi.org/10.3389/fmats.2019.00062.

[35] J.M. Rosas, J. Bedia, J. Rodriguez-Mirasol, T. Cordero, Preparation of Hemp-Derived Activated Carbon Monoliths. Adsorption of Water Vapor, Ind. Eng. Chem. Res. 47 (2008) 1288–1296. https://doi.org/10.1021/ie070924w.
[36] Y. Wang, S. Zuo, J. Yang, S.-H. Yoon, Evolution of Phosphorus-Containing Groups on Activated Carbons during Heat Treatment, Langmuir. 33 (2017) 3112–3122. https://doi.org/10.1021/acs.langmuir.7b00095.
[37] J.L. Figueiredo, M.F.R. Pereira, M.M.A. Freitas, J.J.M. Órfão, Modification of the surface chemistry of activated carbons, Carbon. 37 (1999) 1379–1389. https://doi.org/10.1016/S0008-6223(98)00333-9.
[38] F. Carrasco-Marín, A. Mueden, C. Moreno-Castilla, Surface-Treated Activated Carbons as Catalysts for the Dehydration and Dehydrogenation Reactions of Ethanol, J. Phys. Chem. B. 102 (1998) 9239–9244. https://doi.org/10.1021/jp981861l.
[39] J.M. Rosas, J. Bedia, J. Rodríguez-Mirasol, T. Cordero, HEMP-derived activated carbon fibers by chemical activation with phosphoric acid, Fuel. 88 (2009) 19–26. https://doi.org/10.1016/j.fuel.2008.08.004.
[40] F.J. García-Mateos, R. Ruiz-Rosas, M.D. Marqués, L.M. Cotoruelo, J. Rodríguez-Mirasol, T. Cordero, Removal of paracetamol on biomass-derived activated carbon: Modeling the fixed bed breakthrough curves using batch adsorption experiments, Chem. Eng. J. 279 (2015) 18–30. https://doi.org/10.1016/j.cej.2015.04.144.
[41] M.J. Valero-Romero, F.J. García-Mateos, J. Rodríguez-Mirasol, T. Cordero, Role of surface phosphorus complexes on the oxidation of porous carbons, Fuel Process. Technol. 157 (2017) 116–126. https://doi.org/10.1016/j.fuproc.2016.11.014.
[42] J. Bedia, R. Ruiz-Rosas, J. Rodríguez-Mirasol, T. Cordero, A kinetic study of 2-propanol dehydration on carbon acid catalysts, J. Catal. 271 (2010) 33–42. https://doi.org/10.1016/j.jcat.2010.01.023.
[43] J. Bedia, J.M. Rosas, J. Márquez, J. Rodríguez-Mirasol, T. Cordero, Preparation and characterization of carbon based acid catalysts for the dehydration of 2-propanol, Carbon. 47 (2009) 286–294. https://doi.org/10.1016/j.carbon.2008.10.008.
[44] J. Bedia, R. Barrionuevo, J. Rodríguez-Mirasol, T. Cordero, Ethanol dehydration to ethylene on acid carbon catalysts, Appl. Catal. B Environ. 103 (2011) 302–310. https://doi.org/10.1016/j.apcatb.2011.01.032.
[45] J. Bedia, J.M. Rosas, J. Rodríguez-Mirasol, T. Cordero, Pd supported on mesoporous activated carbons with high oxidation resistance as catalysts for toluene oxidation, Appl. Catal. B Environ. 94 (2010) 8–18. https://doi.org/10.1016/j.apcatb.2009.10.015.
[46] J.M. Rosas, R. Ruiz-Rosas, J. Rodríguez-Mirasol, T. Cordero, Kinetic study of the oxidation resistance of phosphorus-containing activated carbons, Carbon. 50 (2012) 1523–1537. https://doi.org/10.1016/j.carbon.2011.11.030.
[47] M.J. Valero-Romero, E.M. Calvo-Muñoz, R. Ruiz-Rosas, J. Rodríguez-Mirasol, T. Cordero, Phosphorus-Containing Mesoporous Carbon Acid Catalyst for Methanol Dehydration to Dimethyl Ether, Ind. Eng. Chem. Res. 58 (2019) 4042–4053. https://doi.org/10.1021/acs.iecr.8b05897.
[48] A.M. Rao, A.W.P. Fung, M.S. Dresselhaus, M. Endo, Structural characterization of heat-treated activated carbon fibers, J. Mater. Res. 7 (1992) 1788–1794. https://doi.org/10.1557/JMR.1992.1788.

[49] J.A. Moulijn, A. Tarfaoui, F. Kapteijn, General aspects of catalyst testing, Catal. Today. 11 (1991) 1–12. https://doi.org/10.1016/0920-5861(91)87002-5.
[50] J. Bedia, J.M. Rosas, D. Vera, J. Rodríguez-Mirasol, T. Cordero, Isopropanol decomposition on carbon based acid and basic catalysts, Catal. Today. 158 (2010) 89–96. https://doi.org/10.1016/j.cattod.2010.04.043.
[51] D. Barthomeuf, Importance Of The Acid Strength In Heterogeneous Catalysis, in: B. Imelik, C. Naccache, G. Coudurier, Y.B. Taarit, J.C. Vedrine (Eds.), Catal. Acids Bases, Elsevier, 1985: pp. 75–89. https://doi.org/10.1016/S0167-2991(09)60158-0.
[52] R.M. Rioux, M.A. Vannice, Hydrogenation/dehydrogenation reactions: isopropanol dehydrogenation over copper catalysts, J. Catal. 216 (2003) 362–376. https://doi.org/10.1016/S0021-9517(02)00035-0.
[53] S.P. Banzaraktsaeva, E.V. Ovchinnikova, I.G. Danilova, V.V. Danilevich, V.A. Chumachenko, Ethanol-to-ethylene dehydration on acid-modified ring-shaped alumina catalyst in a tubular reactor, Chem. Eng. J. 374 (2019) 605–618. https://doi.org/10.1016/j.cej.2019.05.149.
[54] H.M. Salem, R.S. Mohamed, A.A. Alkahlawy, H.M. Gobara, A.E.A. Hassan, S.A. Hassan, Enhanced ethylene production by dehydration of ethanol over Al/SBA-15 mesoporous catalysts, J. Porous Mater. 26 (2019) 735–745. https://doi.org/10.1007/s10934-018-0670-8.
[55] D. Masih, S. Rohani, J.N. Kondo, T. Tatsumi, Catalytic dehydration of ethanol-to-ethylene over Rho zeolite under mild reaction conditions, Microporous Mesoporous Mater. 282 (2019) 91–99. https://doi.org/10.1016/j.micromeso.2019.01.035.
[56] G. Garbarino, P. Riani, M. Villa García, E. Finocchio, V. Sánchez Escribano, G. Busca, A study of ethanol conversion over zinc aluminate catalyst, React. Kinet. Mech. Catal. 124 (2018) 503–522. https://doi.org/10.1007/s11144-018-1395-z.
[57] P.D. Srinivasan, K. Khivantsev, J.M.M. Tengco, H. Zhu, J.J. Bravo-Suárez, Enhanced ethanol dehydration on γ-Al2O3 supported cobalt catalyst, J. Catal. 373 (2019) 276–296. https://doi.org/10.1016/j.jcat.2019.03.024.
[58] K. Ramesh, L.M. Hui, Y.-F. Han, A. Borgna, Structure and reactivity of phosphorous modified H-ZSM-5 catalysts for ethanol dehydration, Catal. Commun. 10 (2009) 567–571. https://doi.org/10.1016/j.catcom.2008.10.034.
[59] E. Chaichana, W. Wiwatthanodom, B. Jongsomjit, Carbon-Based Catalyst from Pyrolysis of Waste Tire for Catalytic Ethanol Dehydration to Ethylene and Diethyl Ether, Int. J. Chem. Eng. 4102646 (2019) 1–10. https://doi.org/10.1155/2019/4102646.
[60] S. Hassanpour, F. Yaripour, M. Taghizadeh, Performance of modified H-ZSM-5 zeolite for dehydration of methanol to dimethyl ether, Fuel Process. Technol. 91 (2010) 1212–1221. https://doi.org/10.1016/j.fuproc.2010.03.035.
[61] H. Bateni, C. Able, Development of Heterogeneous Catalysts for Dehydration of Methanol to Dimethyl Ether: A Review, Catal. Ind. 11 (2019) 7–33. https://doi.org/10.1134/S2070050419010045.